Energy Syst (2013) 4:219–237
DOI 10.1007/s12667-012-0075-8

ORIGINAL PAPER

A new approach to optimize the operating conditions of a polymer electrolyte membrane fuel cell based on degradation mechanisms

Ramin Roshandel · Tarannom Parhizgar

Received: 20 June 2012 / Accepted: 27 December 2012 / Published online: 31 January 2013

Abstract Performance degradation remains as one of the primary limitations for practical applications of proton exchange membrane (PEM) fuel cells. The performance of a PEM fuel cell stack is affected by many internal and external factors, such as fuel cell design and assembly, degradation of materials, operational conditions, and impurities or contaminants. Performance degradation is unavoidable, but the degradation rate can be minimized through a comprehensive understanding of degradation and failure mechanisms. In present work, a single PEM fuel cell for stationary applications is investigated. Membrane and catalyst layers (anode and cathode electrodes) are considered as critical components that affect the degradation of the cell. The model used in this work diagnoses degradation of MEA (platinum degradation in catalyst layers and membrane thinning and dehydration in polymer membrane), and by considering the degradation over operating time, estimates power density over system lifetime. In this paper, also three optimization model with different objective functions are developed tomaximize total energy production. The results show that by continuously optimizing the operating conditions, total energy generation of the system will increase up to 3.16 %.

Keywords Energy systems · PEM fuel cell · Degradation model · Operation condition · Optimization

R. Roshandel (✉) · T. Parhizgar
Department of Energy Engineering, Sharif University of Technology,
Azadi Avenue, P.O. Box 11365-9567, Tehran, Iran
e-mail: Roshandel@sharif.edu

1 Introduction

Extending fuel cell total energy (kw.hr energy produced during fuel cell lifetime) is a necessary objective for reducing fuel cell per unit electricity cost. Total generated energy is increased by extending life time and operating at maximum possible output power. Fuel cell life time and output power are affected by degradation mechanisms. Reducing the rate of degradation mechanisms can be achieved by implementing an appropriate optimization strategy that prevents the system from being placed in the operating regions that cause failure. To obtain the optimization strategy, first a degradation model is developed. The degradation procedure of fuel cell stack components and its impact on electricity generation through the remaining lifetime, in most cases, has been insufficiently understood. The lengthy required testing time, lack of understanding of most degradation mechanisms, the difficulty of performing in-situ, and non-destructive structural evaluation of key components make the issue difficult to investigate. The fuel cell membrane electrode-assembly (MEA) plays a vital role in the overall lifetime achieved by a stack [1]. MEA is the main component of our study. Our approach to improve PEM fuel cell total energy production is to investigate the degradation mechanisms and optimizing operating conditions which maximize cell total energy regarding degradation mechanisms. The MEA performance shows degradation over operating time, which is dependent upon fuel cell design and assembly, degradation of materials, operational conditions and impurities or contaminants. To model the degradation mechanisms, it is necessary to understand degradation processes of the PEMFC components. Various studies have been conducted in this field. Their differences are mostly in studied components, experimental or model based degradation diagnosis and the purpose of degradation diagnosis. Borup et al. [2] made a review on PEM fuel cell components (membrane, electrodes and bipolar plates) degradation. In this review, some of the targets for PEM fuel cell systems, as indicated by the US DOE (Department of Energy) and Japanese NEDO (New Energy & Industrial Technology Development Organization) are presented showing the importance of PEM fuel cell degradation research. The purpose of their paper is to investigate the effects of operating conditions (Impurity and Subfreezing) on fuel cell durability using experimental data of durability tests. Yousfi et al. [3] reviewed PEM fuel cell catalyst degradation using available experimental research. In their paper, the effect of fuel and oxidant starvation on catalyst and carbon support degradation is investigated and some characterization methods or mitigation strategies for catalyst layer are presented to build catalyst illustrative fault tree. Darling et al. [4] developed a mathematical model of oxidation and dissolution of supported platinum catalysts in PEM fuel cells to study electrode potential and particle size effects on catalyst stability. Chen et al. [5] studied membrane degradation. In their study, experimental degradation data are collected, the membrane samples are analyzed, and the effects of Fe^{2+} concentration and temperature on membrane degradation are discussed. In their dissertation, both experimental and modeling methods are applied to investigate the chemical durability of PFSA membranes for fuel cell applications. Bruijn et al. [6] reviewed the degradation mechanisms of membranes, electrodes, bipolar plates and seals. In their study, by collecting long-term experiments, the relation between degradation mechanisms and the operating conditions (voltage, pressure, humidity and temperature) was discussed.

Schmittinger et al. [7] presented the effect of humidity on fuel cell components (catalyst layers, the gas diffusion media and the membrane) degradation in long term performance. The proposed research shows that the main cause of short life and performance degradation is poor water management. Jayson et al. [8] optimized peroxide mitigation strategies, mechanically reinforced membrane and chemically stabilized membrane by decreasing cost and performance impact. They try to improve the lifetime of PEM for fuel cell by seeking technologies that will prevent membrane failure.

In the present work, unlike the previous studies, membrane and catalyst degradation that are dominant, especially in stationary applications are modeled simultaneously, and the effects of temperature, humidity, and pressure on degradation mechanisms are investigated.

In most researches, optimum technologies and structure parameters regarding cost and performance degradation are obtained whilein this paper structure parameters has been fixed and the effect of operational conditions on degradation mechanisms is discussed. To do this, a model has been developed which includes membrane chemical degradation, platinum growth in catalyst layer and electrode reduction in active surface area. Using degradation model, voltage and current are estimated as a function of catalyst and membrane degradation. Degradation itself is expressed as a function of operating conditions. Afterwards, by optimizing with three objective functions the optimal operation conditions which maximize power output through fuel cell life time are presented.

In short, the main innovations in this paper include:

- A dynamic model which considers the decreases in catalyst active surface area and the membrane thinning simultaneously
- The effect of membrane and catalyst degradation on fuel cell performance
- Optimized operational conditions to maximize the total energy over fuel cell life time regarding degradation mechanisms
- History based optimization strategy that maximize system total energy.

2 Mathematical modeling

2.1 Performance modeling

The general performance model which is used in most researches to estimate fuel cell performance is presented in Eqs. 1–2 [9]. In this model degradation are not considered. Therefore, equations are time independent. The fuel cell output power density is calculated as Eq. 1.

$$P = V_{fc} \times i \tag{1}$$

where output voltage (V) of PEM fuel cell is greatly affected by Ohmic, concentration, and activation polarizations. The operating cell potential can be formally expressed as Eq. 2. Related terms are presented in Table 1 [10].

$$V_{fc} = V_{rev} - V_{ohm} - V_{act} - V_{conc} \tag{2}$$

Table 1 Voltage term equations

Voltage terms	Equation	
V_{rev}	$1.229 + (4.308 \times 10^{-5})T \times \ln\left[P_{H_2}(P_{O_2})^{\frac{1}{2}}\right] - (8.453 \times 10^{-4})(T - 298.15)$	(3)
V_{ohm}	$i \times t_m \frac{181.6\left[1+0.03i+0.062(\frac{T}{303})^2 i^{2.5}\right]}{(\lambda-0.634-3i)\exp\left[4.18(\frac{T-303}{T})\right]}$	(4)
$V_{cross\&act}$	$\frac{RT}{\alpha nF} \ln\left(\frac{i+i_{H2}^{cross}}{i_0}\right)$	(5)
V_{conc}	$\frac{RT}{nF}\left(1+\frac{1}{\alpha}\right)\frac{i_L}{i_L-i}$	(6)

2.2 Degraded performance modeling

As fuel cell works, due to chemical reactions, degradation occurs. Degradation affects fuel cell performance. In this section, a new model is developed which considers degradation effects on fuel cell performance. Considering degradation makes equations time dependent.

Recognition of degradation mechanisms and their dependence on operation condition is critical for understanding fuel cell longterm performance. In order to determine power density through time, the value of the voltage and current regarding degradation should be estimated as the function of time. Power density through fuel cell life time can be expressed as Eq. 7.

$$P(t) = V_{fc}(t) \times i(t) \tag{7}$$

2.2.1 Voltage degradation

In degraded performance model, overpotentials are time dependent and can be expressed in following equations.

$$V_{fc}(t) = V_{rev} - V_{ohm}(t) - V_{cross\&act}(t) - V_{conc} - V_{ECSA}(t) \tag{8}$$

Degradation model of over potentials is developed based on components degradation; all losses are functions of the catalyst and membrane degradation.

Ohmic loss Ohmic loss in PEM fuel cell is caused by resistance to hydrogen ions transition and is calculated as follow [11]:

$$V_{ohm}(t) = i \times r_{ion}(t) \tag{9}$$

$$r_{ion}(t) = t_m(t)\frac{181.6\left[1 + 0.03i + 0.062(\frac{T}{303})^2 i^{2.5}\right]}{(\lambda - 0.634 - 3i)\exp\left[4.18(\frac{T-303}{T})\right]} \tag{10}$$

Ionic resistance is totally dependent on membrane water content and membrane thickness. In Eq. 10, λ, represent membrane water contentwhich shows number of

water molecules with respect to SO^{3-} molecules in membrane [12]. λcan be related to membrane relative humidity (RH) using Eq. 11[13].

$$\lambda = (0.043 + 17.81RH - 39.85RH^2 + 36.0RH^3) \tag{11}$$

Here, is assumed that membrane relative humidity is equal to average of anode and cathode relative humidity. Relative humidity is estimated using Eq. 12.

$$RH = \frac{P_v}{P_{sat}} \tag{12}$$

Polymer electrolyte membrane thickness decreases during fuel cell life time. Different phenomena can cause membrane thinning. The most common reason is chemical degradation. It has been proposed that carboxylic end groups left over from the Nafion manufacturing process may be susceptible to attack by radical species generated during fuel cell reactions. The proposed mechanisms are as follows:

Step 1: $\text{R-CF}_2\text{ COOH} + \text{OH}^{\cdot} \rightarrow \text{R-CF}_2\cdot + \text{CO}_2 + \text{H}_2\text{O}$
Step 2: $\text{R-CF}_2^{\cdot} + \text{OH}^{\cdot} \rightarrow \text{R-CF}_2\text{OH} \rightarrow \text{R-COF} + \text{HF}$
Step 3: $\text{R-COF} + \text{H}_2\text{O} \rightarrow \text{R-COOH} + \text{HF}$

Hydrogen peroxide which is an intermediate of the electrochemical oxygen reduction reaction forms the radical species, such as hydroxyl radicals, also hydrogen or oxygen permeating to the anode catalyst layer may react and produce peroxide species. Produced radicals cause membrane thinning, release of fluoride ions, increased gas crossoverand consequently voltage degradation.

Membrane thickness as the function of time through fuel cell lifetime is presented in Eq. 13 [14].

$$t_m(t) = \left(\frac{1}{2}t_m^0 + 1\right) f(t) \tag{13}$$

Fraction of remaining electrolyte ($f(t)$) is proportional to hydrogen cross over according to Eq. 14 [14].

$$-\frac{df(t)}{dt} = K_1 \times N_{H_2}(t) \times f(t) \tag{14}$$

Hydrogen crosses over current is related to membrane permeability and hydrogen-partial pressure as Eq. 16 [15].

$$i_{H_2}^{cross}(t) = 2FN_{H_2}(t) \tag{15}$$

$$i_{H_2}^{cross}(t) = \left(\frac{P_{M,H_2}}{t_m(t)}\right) P_{H_2}^a \tag{16}$$

Finally, hydrogen partial pressure and membrane permeability is determined according to Eqs. 17 and 18 [15].

$$P^a_{H_2} = \left(\frac{P^a_{H_2-inlet}}{P^a_{inlet}}\right)\left(\frac{P^a_{inlet}+P}{2}\right) \tag{17}$$

$$P_{M,H_2} = 1.39\times10^{-7}e^{-2980/T} \tag{18}$$

According to above explanation, the dependency of Ohmic loss to temperature, relative humidity, cell current and fraction of remaining electrolyte is expressed by Eq. 19.

$$V_{ohm}(t) = \frac{181.6i\times(0.5t^0_m+1)f(t)\left[1+0.03i+0.062(\frac{T}{303})^2i^{2.5}\right]}{((0.043+17.81RH-39.85RH^2+36.0RH^3)-0.634-3i)\exp\left[4.18(\frac{T-303}{T})\right]} \tag{19}$$

Crossover and activation loss As any polymer membrane, the polymer electrolyte of a fuel cell allows some gas to permeate across it. Crossover rates of different gases have been measured for Nafion membranes and can be broadly described by Fick's law. Hydrogen crossover to cathode incurs accelerating degradation mechanisms; in addition its effect on performance loss is added to activation losses, as shown in Eq. 20 [16,17].

$$V_{cross\&act}(t) = \frac{RT}{\alpha nF}\ln\left(\frac{i+i^{cross}_{H2}(t)}{i_0}\right) \tag{20}$$

The correlation between $V_{cross\&act}(t)$and operations conditions is presented as Eq. 21.

$$V_{cross\&act}(t) = \frac{RT}{anF}\ln\left(\frac{1}{i_0}\times\left(i+\left(\frac{1.39\times10^{-7}e^{\frac{-2980}{T}}}{(\frac{1}{2}t^0_m+1)f(t)}\right)\left(\frac{P^a_{H_2-inlet}}{P^a_{inlet}}\right)\left(\frac{P^a_{inlet}+P}{2}\right)\right)\right) \tag{21}$$

Electrochemical active surface area loss One critical issue that affects voltage loss during PEM fuel cells operating lifetime is the electrochemical active surface area (ECSA) loss of carbon supported platinum nanoparticles at the cathode. The decrease in the electrochemical active surface area (ECSA) is corresponded to voltage loss by the Eq. 22. a_0 and $a(t)$ are the ECSA at the beginning and at time t of fuel cell lifetime, respectively [6,18].

$$V_{ECSA}(t) = \frac{RT}{\alpha nF}\ln\left(\frac{a_0}{a(t)}\right) \tag{22}$$

Considering constant platinum (Pt) mass in electrodes, the correlation between Pt diameter and electrochemical active surface area is expressed by Eq. 23. r_0 and $r(t)$ represent the particle initial radius and the particle radius at time t respectively [5]:

$$\%A_{ECSA} = \frac{a(t)}{a_0} = \frac{r_0}{r(t)} \tag{23}$$

Platinum radius changes mainly because of Pt dissolution and deposition in the catalysts. Four reactions lead to Pt dissolution and deposition. In the present study, active surface area degradation is modeled considering following reactions [19]:

- Reaction 1: Pt electrochemical dissolution

$$\mathrm{Pt} \rightarrow \mathrm{Pt}^{2+} + 2\mathrm{e}^{-} (U_1^0 = 1.188\,\mathrm{V})$$

- Reaction 2: Pt oxidation

$$\mathrm{Pt} + \mathrm{H_2O} \rightarrow \mathrm{PtO} + 2\mathrm{H}^{+} + 2\mathrm{e}^{-} (\mathrm{U}_2^0 = 0.98\,\mathrm{V})$$

- Reaction 3: Diffusion of Pt ions and subsequent precipitation by hydrogen reduction

$$\mathrm{Pt}^{2+} + \mathrm{H_2} \rightarrow \mathrm{Pt} + 2\mathrm{H}^{+}$$

- Reaction 4: Chemical dissolution of Pt oxide

$$\mathrm{PtO} + 2\mathrm{H}^{+} \rightarrow \mathrm{Pt}^{2+} + \mathrm{H_2O}$$

Last two reactions are not considered due to small rate of reaction 3 and the unclear kinetics of reaction 4. What is more, inclusion of proposed reactions does not affect the results measurably due to their slow kinetics [2].

According to Pt dissolution and deposition reactions rate, Pt particle radius presented as Eq. 24 [2]:

$$\frac{dr(t)}{dt} = -\frac{M}{\rho}(r_1(t) + r_2(t)) \tag{24}$$

In Eq. 24, $r_1(t)$ and $r_2(t)$ represent the rate of first and second reactions. $r_1(t)$is calculated as Eq. 25 [15].

$$r_1(t) = k_1(1 - \theta_{PtO}(t))\left[\exp\left(\frac{\alpha_{a,1} n_1 F}{RT}(\phi_1 - \phi_2 - U_1(t))\right)\right. \\ \left. -\left(\frac{c_{pt^{2+}}}{c_{Pt^{2+},ref}}\right)\exp\left(-\frac{\alpha_{c,1} n_1 F}{RT}(\phi_1 - \phi_2 - U_1(t))\right)\right] \tag{25}$$

where $\theta_{PtO}(t)$ is the fraction of platinum surface covered by PtO and is obtained as Eq. 26.

$$\frac{d\theta_{PtO}(t)}{dt} = \left(\frac{r_2(t)}{\Gamma_{\max}}\right) - \left(\frac{2\theta_{PtO}(t)}{r(t)}\right)\frac{dr(t)}{dt} \tag{26}$$

$U_1(t)$ is the standard equilibrium potential of reaction 1 [2].

$$U_1(t) = U_1^0 - \frac{\Delta\mu_{Pt}(t)}{2F} \tag{27}$$

Standard equilibrium potential is shifted away from the literature value for bulk platinum by the factor $\Delta\mu_{Pt}(t)$. The proposed factor accounts for the effect of surface tension of the platinum crystallite on standard equilibrium potential.

$$\Delta\mu_{Pt}(t) = \frac{\sigma_{Pt} M_{Pt}}{r(t)\rho_{Pt}} \tag{28}$$

The rate of second reaction is formulated as Eqs. 29–31, [2].

$$r_2(t) = k_2 \left[\exp\left(-\frac{\omega\theta_{PtO}(t)}{RT}\right) \exp\left(\frac{\alpha_{a,2} n_2 F}{RT}(\phi_1 - \phi_2 - U_2(t))\right) - \theta_{PtO}(t)\left(\frac{c_{H^+}^2}{c_{H^+,ref}^2}\right) \exp\left(-\frac{\alpha_{c,2} n_2 F}{RT}(\phi_1 - \phi_2 - U_2(t))\right)\right] \tag{29}$$

$$U_2(t) = U_2^0 + \frac{\Delta\mu_{PtO}(t)}{2F} - \frac{\Delta\mu_{Pt}(t)}{2F} \tag{30}$$

$$\Delta\mu_{Pto}(t) = \Delta\mu_{P_{tO}}^{O} + \frac{\sigma_{PtO} M_{PtO}}{r(t)\rho_{PtO}} \tag{31}$$

Active surface area loss during fuel cell life time is a function of temperature and Pt particles radius through time as is expressed in Eq. 32. Pt particles radius depends on its initial radius, cell potential and electrochemical reactions rate.

$$V_{ECSA}(t) = \frac{RT}{\alpha n F} \ln\left(\frac{r(t)}{r_0}\right) \tag{32}$$

Therefore, the degraded output voltage can be calculated by Eqs. (3, 6, 15, 21, 32).

2.2.2 Current kinetic model

During fuel cell operation, active surface area and hydrogen cross over current density increase. Therefore, net accessible current density during time, decreases as Eq. 33. In other words, if a fixed output current is desired, during operation, supply mass flow rate should increase [20].

$$i(t) = i \times (1 - \theta_{PtO}(t)) - i_{H2}^{cross}(t) \tag{33}$$

Using equations in section (a), current density through time can be estimated as a function of temperature, pressure, fraction of remaining electrolyte and fraction of platinum surface covered by PtO (Eq. 34).

$$i(t) = i \times (1 - \theta_{PtO}(t)) - \left(\frac{1.39 \times 10^{-7} e^{\frac{-2980}{T}}}{(\frac{1}{2}t_m^0 + 1) f(t)}\right)\left(\frac{P^a_{H_2-inlet}}{P^a_{inlet}}\right)\left(\frac{P^a_{inlet} + P}{2}\right) \tag{34}$$

3 Optimization

The optimization objective is to maximize total energy production regarding degradation mechanisms. Optimization model find the operating conditions which minimize the per unit energy cost. The decision variables which affect the power generation are cell temperature, anode and cathode relative humidity, as well as anode and cathode fuel pressure. The optimization model is also subject to several constraints. It is assumed that PEM fuel cell is designed to work in the specific temperature and pressure ranges. The proposed constraints are expressed in Eqs. 35–39.

$$T_{Min} \leq T \leq T_{Max} \tag{35}$$

$$P_{anode,Min} \leq P_{anode} \leq P_{anode,Max} \tag{36}$$

$$P_{cathode,Min} \leq P_{cathode} \leq P_{cathode,Max} \tag{37}$$

$$RH_{cathode,Min} \leq RH_{cathode} \leq RH_{cathode,Max} \tag{38}$$

$$RH_{anode,Min} \leq RH_{anode} \leq RH_{anode,Max} \tag{39}$$

Three objective functions are presented to compare the effect of controlling operational conditions on fuel cell power generation and degradation mechanisms. In each proposed strategy, decision variables and constraints are the same but optimization objective functions are different. In this study, the objective function is based on both degradation and electrochemical phenomena; therefore, the effect of increasing of performance and cell degradation is estimated simultaneously. In the other words, no weighted methods are needed in our optimization formulation.

3.1 Objective function 1

Here, power density is maximized at the initial time (t_0) of fuel cell operation. In other words, degradation mechanism rate and power losses due to the degradation have been ignored. The operational conditions are constant through fuel cell lifetime.

$$Max\, P(t_0) = Max\, V(t_0) \times I(t_0) \tag{40}$$

3.2 Objective function 2

To determine the operational conditions that maximize system total energy in 10,000 h of fuel cell lifetime, the second objective function is applied on the developed model as Eq. 41. In this strategy, the optimum operational conditions are obtained at the initial time and they are constant through fuel cell lifetime.

$$Max \int_{t_0}^{t_{10,000}} P(t) \cdot dt = Max \int_{t_0}^{t_{10,000}} V(t) \times I(t) \cdot dt \tag{41}$$

3.3 Objective function 3

In this strategy, power density is maximized in every time step of fuel cell lifetime. It is clear that the operational conditions may be changed continuously through time. Equation 42 presents the third objective function:

$$Max\, P(t) = Max\, V(t) \times I(t) \tag{42}$$

3.4 Optimization procedure

Figure 1 points out the procedure of system optimization regarding degradation. The degradation rates are considered to determine the optimum values of pressure, temperature and humidity through fuel cell life time. Genetic algorithm is used and the optimum operation conditions for each objective function are obtained.

4 Validation

To solve a system of Eqs. 1–34, the fourth order Runge–Kutta method is used and the system variables are found. For validation, it should be noted that at present, the voltage degradation curve is the only experimental piece of data available in the literature that considers implicit degradation mechanisms. Therefore, voltage degradation curve is commonly used to validate the agreement between the model and experiments. Model results are verified with experimental results (at the operating conditions T = 348 K, $P_{anode} = P_{cathode} = 1$ bar, $RH_{anode} = RH_{cathode} = 70$ %) provided by S. Higashiguchi et al. [21]. According to Fig. 2, degradation curve of cell potential versus long runtime for the model is in good agreement with the experimental curve. For validation output power through time regarding degradation, Fowler [22]presented power density at discrete points of fuel cell lifetime (at the operating conditions T = 353 K, $P_{anode} = P_{cathode} = 3$bar, $RH_{anode} = RH_{cathode} = 100$ %), the comparison is also presented in Table 2. As can be seen, the model results are nearly close to the experimental data provided by Fowler [22].

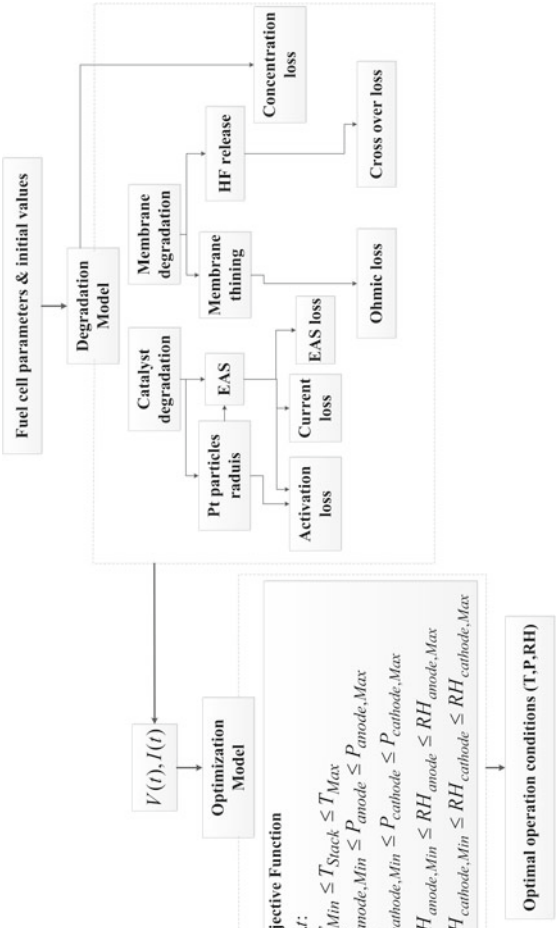

Fig. 1 Flow diagram of the developed optimization model

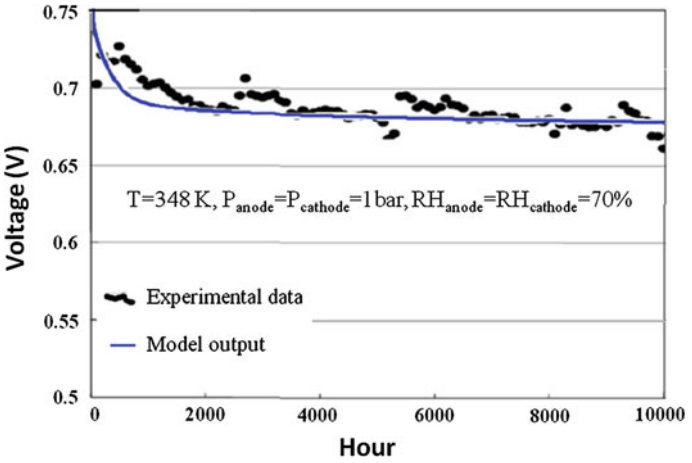

Fig. 2 Comparison between the modeling and experimental results for output voltage in PEM fuel cell life time

Table 2 Comparison between the modeling and experimental results for power density degradation in PEM fuel cell

Time (h)	Model output (power density W/cm^2)	Power density decrement (%) (model output)	Power density decrement (%) (experimental date)
0	0.765	0	0
1,500	0.6837	11	14
3,000	0.6454	16	19
4,500	0.612	21	23
6,000	0.5833	25	28

5 Results and discussion

To investigate the effects of operation conditions on cell performance loss due to system degradation, the proposed model is applied to the case study (T = 348 K, $P_{anode} = P_{cathode} = 1$ bar, $RH_{anode} = RH_{cathode} = 70$ %). Figures 3 and 4 present the main output of degradation model for the case study. Figure 3 presents the increment of degradation mechanisms. Three important observations stand out from Fig. 3: first, at the beginning of fuel cell operation lifetime the loss of active surface area is dominant; second, membrane degradation rate increases linearly during fuel cell lifetime; third, the catalyst degradation is almost more significant through fuel cell life time.

Figure 4 indicates the behavior of output voltage and power density through the fuel cell lifetime. The rates of voltage and power density degradation are almost the same through fuel cell life time. It is also found that, after 10,000 h of operation, 22 % power density and approximately 9 % output voltage are decreased.

The base case parameters are presented in Table 3. Figure 5 presents the optimum temperature for proposed objective functions through the time. For the first objective function which considers the maximum power density regardless degradation

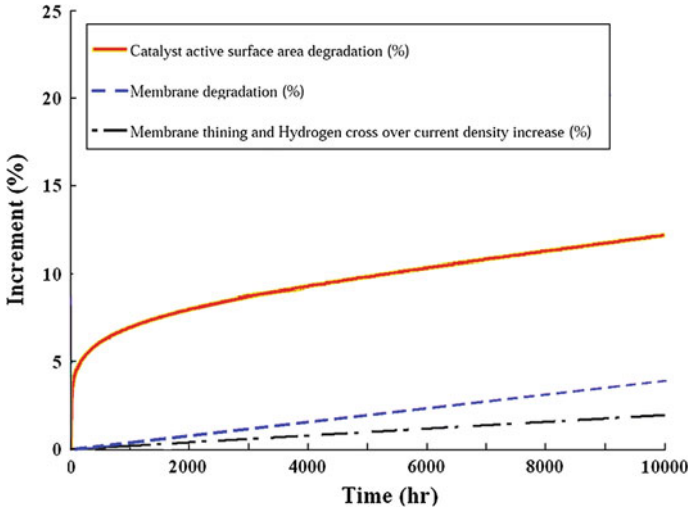

Fig. 3 Degradation rate in PEM fuel cell lifetime

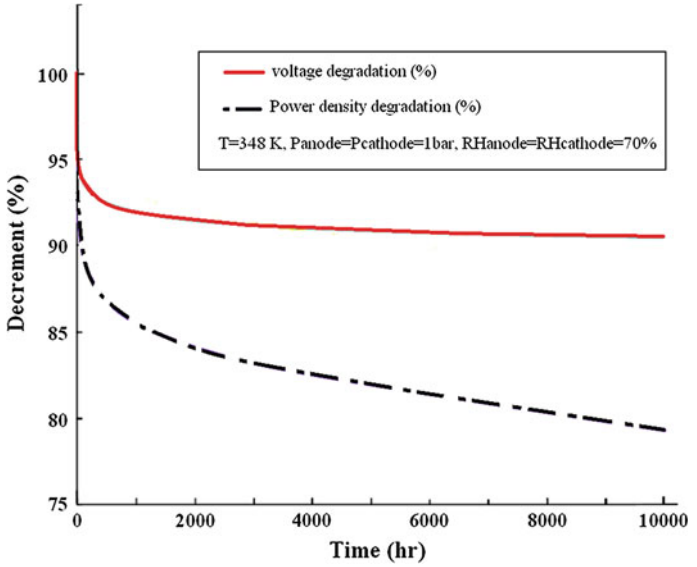

Fig. 4 Voltage and power losses in PEM fuel cell lifetime

mechanisms the maximum operating temperature is resulted. However, for second objective function the optimum temperature is decreased to minimize degradation rate which results in increase in total energy output of fuel cell. For third objective function the optimum temperature is determined for any desired time through fuel cell life time. The results show that the optimum operating temperature is decreased as fuel cell suffers degradation through time.

Table 3 Value of constants in optimization model

Parameter	Value	Unit
T_{Max}	373	K
T_{Min}	313	K
$P_{anode,Max}$	3	bar
$P_{anode,Min}$	1	bar
$RH_{anode,Max}$	100 %	–
$RH_{anode,Min}$	0 %	–
$RH_{cathode,Max}$	100 %	–
$RH_{cathode,Min}$	0 %	–
$P_{cathode,Max}$	3	bar
$P_{cathode,Min}$	1	bar
t_0	0	h
$t_{10,000}$	10,000	h

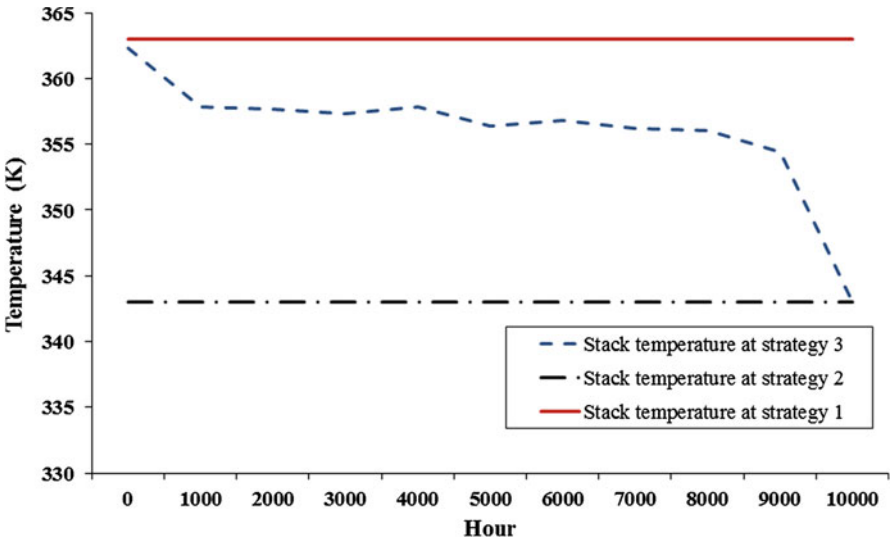

Fig. 5 Temperature behavior in 10,000 h of fuel cell operation time in different strategies

It can be infer from Fig. 6, that the anode and cathode optimum operating pressure are the same for all objective functions. It is also found that the cathode optimum operating pressure is higher due to water management considerations.

Figure 7 presents the optimum humidity behavior in the three strategies. Inthe first objective functionsaturated situation is suggested. This is mainly due to maximum membrane ionic conductivity in saturated membrane. In the second objective function, to minimize degradation due to hydrogen cross over lower relative humidity at anode and cathode is proposed. In other words, lower humidity causes less reaction on catalyst and causes lower catalyst degradation [15]. In third objective function the

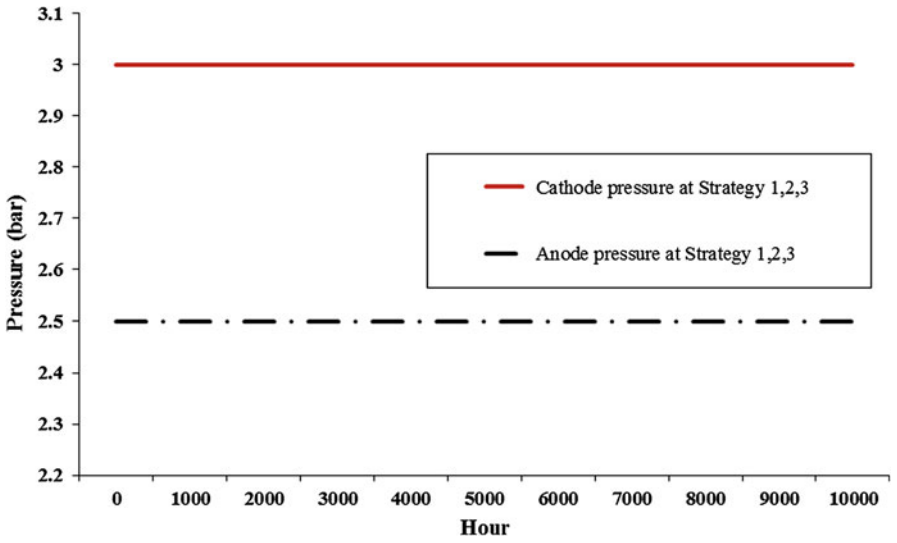

Fig. 6 Pressure behavior in 10,000 h of fuel cell operation time in different strategies

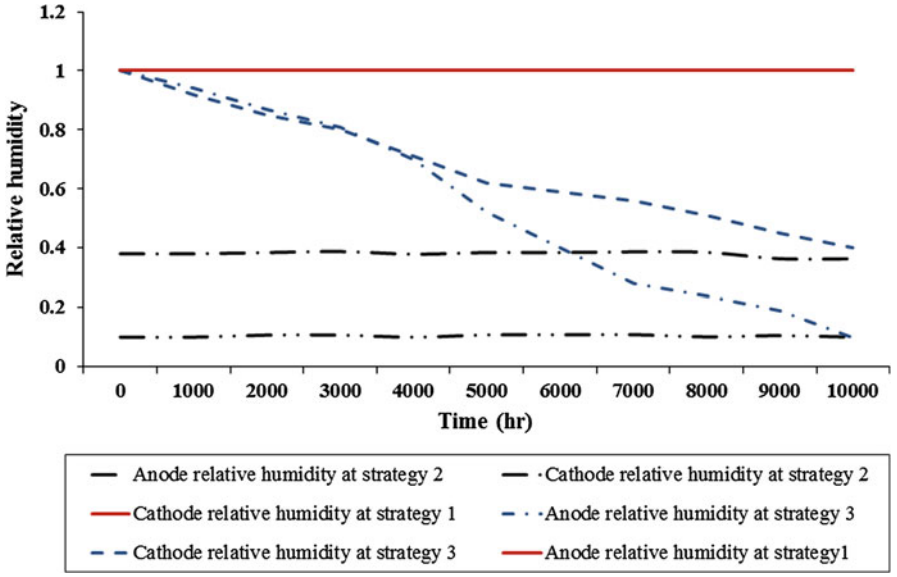

Fig. 7 Humidity behavior in 10,000 h of fuel cell operation time in different strategies

optimum humidity is continuously decreased through time. It indicates that in long term applications the optimum humidity should be lower than saturated condition to avoid significant performance degradation.

Figure 8 shows the behavior of fuel cell maximum power density through time. In the first objective function, power density is the most at initial time, but degraded drastically over time. In the second objective function regarding considered degradation,

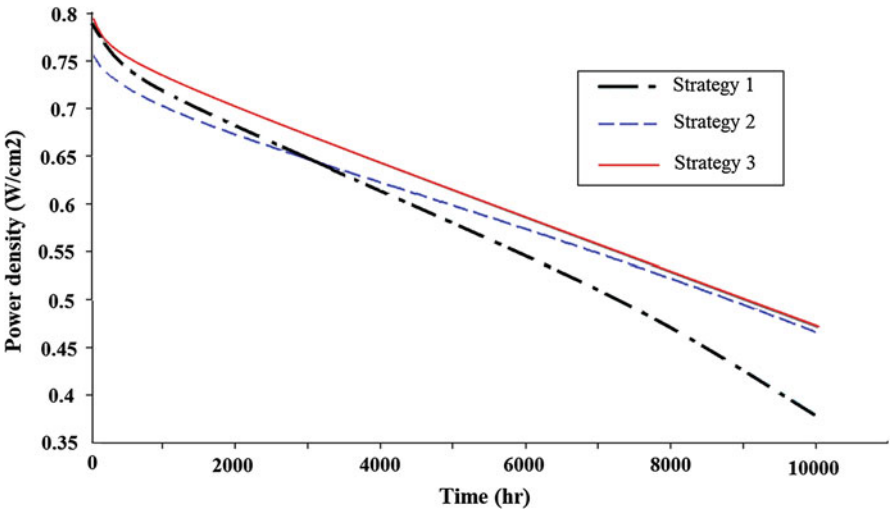

Fig. 8 Power density in fuel cell operational life time in different strategies

Table 4 Life expectancy of three strategies at specific degradation percentage

Membrane degradation (%)	Life expectancy			Catalyst layer degradation (%)	Life expectancy		
	Strategy 1	Strategy 2	Strategy 3		Strategy 1	Strategy 2	Strategy 3
8	5,100	6,200	5,600	15	100	1,500	200
10	6,500	8,000	7,000	20	280	4,700	700
12	8,100	10,000	8,900	25	1,400	10,000	2,200

the maximum power density, is lower at initial time. However, the total energy over time is higher in comparison with the first objective function. In the third objective function, the maximum power density is evaluated in every desired time. Therefore, the total energy over time is much higher than the first and second objective functions. As the result, the total energy of system for third objective function is estimated to be 5.64 kW hr/cm^2, which means 3.16 % higher in comparison with first objective function.

It would be of interest if the optimization model is formulated to predict the life expectancy of fuel cell. To reach particular membrane and catalyst degradation, life expectancy of fuel cell at each strategy is presented in Table 4.

6 Conclusion

In this paper, a degradation model is developed to predict the effects of degradation on PEM fuel cell performance. The results indicate that through fuel cell lifetime, loss of catalyst active surface area is the main degradation mechanism, which directly affects voltage and power density loss. Moreover, operational conditions have a significant

impact on degradation. In the present work, three optimization strategies for maximizing fuel cell electricity generation through lifetime by controlling operating conditions were compared. The objective function which optimizes the operating conditions in each time interval shows higher produced total energy. The optimal operating conditions are expressed as a function of time. It is found that by continuously optimizing the operating conditions, total energy generation of the system will increase up to 3.16 %. This study focused only on degradation mechanisms occurs atstationary applications of PEM fuel cell. In future works, a detailed comprehensive analysis of other degradation mechanisms will be discussed.

Appendix: Nomenclature

Model variables and constants

C_{Ref}	mol m^{-3}	Concentration refrence value (1 M = 1,000 mol m^{-3})
F	C $equiv^{-1}$	Faraday's constant (96.485 C $equiv^{-1}$)
k_1	mol $m^{-2}s^{-1}$	Pt dissolution reaction rate constant
k_2	mol $m^{-2}s^{-1}$	Pt oxidation reaction rate constant
M	kg	Total Pt mass in cathode
M_{Pt}	kg mol^{-1}	Pt molecular weight (0.1951 kg mol^{-1})
M_{PtO}	kg mol^{-1}	PtO molecular weight (0.2110 kg mol^{-1})
n_1	equiv mol^{-1}	Number of equivalent electrons Transferred per mole of Pt dissoluted (2 equiv mol^{-1})
n_2	equiv mol^{-1}	Number of equivalent electrons Transferred per mole of Pt oxidized (2 equiv mol^{-1})
R	J $(mol\ K)^{-1}$	Universal gas constant (8.314 J mol^{-1} K^{-1})
t	S	Time
α_{1a}	Unitless	Cathodic transfer coefficient of Pt dissolution reaction
α_{2a}	Unitless	Anodic transfer coefficient of Pt oxidation reaction
α_{2C}	Unitless	Cathodic transfer coefficient of Pt oxidation reaction
U_1^0	V	Standard thermodynamic potential of Pt dissolution (1.188 V)
U_2^0	V	Standard thermodynamic potential of Pt oxidation (0.980 V)
$+_{max}$	mol m^{-2}	Maximum oxide at Pt surface 2.18e^{-5}(atom ratio of PtO = 1:1)
$\Delta\mu_{Pt}^0$	J mol^{-1}	Fitted chemical potential shift for Pt
ρ_{Pt} , ρ_{PtO}	Kg m^{-3}	Pt metal density (21.090 kg m^{-3}), PtO density (14.100 Kg m^{-3})
θ_{PtO}	Unitless	fraction of platinum surface covered by PtO
σ_{Pt}	J mol^{-2}	Surface tension of Pt nanoparticles (2.37 J m^{-2})
σ_{PtO}	J mol^{-2}	Surface tension of PtO nanoparticles (1.00 J m^{-2})
N_{OH}	mol s^{-1}	Rate at which radicals are produced
N_{H2}	mol s^{-1}	Flux of hydrogen permeating through the membrane
F	Unitless	Fraction of remaining electrolyte
Ω	J mol^{-1}	PtO–PtO interaction coefficient
K_1	mol^{-1}	Proportionality constant (1.8e^{-4} mol^{-1})
K_2	mol cm^{-2}	Proportionality constant (1.8e^{-4} mol^{-1})
$P_{M,H2}$	A cm $cm^{-2}bar^{-1}$	Permeability of the membrane
ΔP_{H2}	bar	Partial pressure difference across the membrane
$i_{cross}^{H_2}$	Mol $cm^{-2}s^{-1}$	H_2 Crossover rate
r_{ion}	Ω	Membrane ionic resistance
t_m	cm	Membrane initial thickness (1.5e^{-3}cm)
Λ	Unitless	Membrane water content

a	Unitless	Membrane relative humidity
l_d	cm	Diffusion layer thickness ($7.5e^{-4}$ cm)
σ_d	$\mathrm{cm}\,\Omega^{-1}$	Diffusion layer electronic conductivity
I	A cm^{-2}	Output current density
i_n	A cm^{-2}	Internal current density related to internal current losses
i_0	A cm^{-2}	Exchange current density related to activation losses
P	bar	Fuel cell backpressure
RH	Unitless	Relative humidity
i_L	A cm^{-2}	Limiting current density
T	K	Fuel cell temperature
P_v	bar	Saturated vapor pressure at humidifier temperature
P_{sat}	bar	Saturated pressure
V_{fc}	V	Fuel cell output voltage
V_{rev}	V	Reversible voltage of fuel cell
V_{ohm}	V	Ohmic loss
$V_{CrossOver}$	V	Activation and cross over loss
$V_{MassTransfer}$	V	Concentration loss
$P_{\mathrm{a}}^{\mathrm{H_2}}$	bar	H_2 Partial pressure
$P_{\mathrm{a}}^{\mathrm{inlet}}$	bar	Fuel cell anode inlet total pressure
$P_{\mathrm{a}}^{\mathrm{H_2}\text{-}inlet}$	bar	H_2 Partial pressure in the inlet stream
P_{O2}, P_{H2}	bar	Partial pressure of oxygen, partial pressure of hydrogen

References

1. Wang, Y., Chen, K.S., Mishler, J., Cho, S.C., Cordobesadroher, X.: A review of polymer electrolyte membrane fuel cells: Technology, applications, and needs on fundamental research. Appl. Energy **88**(4), 981–1007 (2011)
2. Borup, R., Meyers, J., Pivovar, B., Kim, Y.S., Mukundan, R., Garland, N.: Scientific aspects of polymer electrolyte fuel cell durability and degradation. Am. Chem. Soc. **107**, 3904–3951 (2007)
3. Yousfi, N., Moçotéguy, Ph, Candusso, D., Hissel, D.: A review on polymer electrolyte membrane fuel cell catalyst degradation and starvation issues: Causes, consequences and diagnostic for mitigation. Power Sources **194**(1), 130–145 (2009)
4. Darling, R.M., Meyer, J.P.: Kinetic model of platinum dissolution in PEMFCs. Electrochem. Soc. **150**(7), 1523–1527 (2003)
5. Chen, Ch.: Membrane degradation studies in PEMFCs.A Dissertation Presented to the Academic Faculty School of Chemical & Biomolecular Engineering Georgia Institute of Technology (2009)
6. Bruijn, F.A., Dam, V.A., Janssen, G.J.: Review: Durability and degradation issues of PEM fuel cell components. Inter Sci. **8**(1), 3–22 (2008)
7. Schmittinger, W., Vahidi, A.: A review of the main parameters influencing long-term performance and durability of PEM fuel cells. Power Sources **180**(1), 1–14 (2008)
8. Jayson, W., Bauman, K., Kumar, S., Escobedo, G.: Enabling Commercial PEM Fuel Cells with Breakthrough Lifetime Improvements, DOE Hydrogen Program, Progress Report (2005)
9. Pukrushpan, J.T., Peng, H., Anna, G.: Control oriented modeling and analysis for automotive fuel cell systems. ASME **126**, 14–25 (2004)
10. Berger, C.: Handbook of Fuel Cell Technology. Prentice Hall, New York (1968)
11. Costa, R.A., Camacho, J.R., Guimarães S.C. Jr, Salerno, C.H.: The polymer electrolyte membrane fuel cell as electric energy source, steady state and dynamic behavior. School of Electrical Engineering (2004)
12. Santarelli, M.G., Torchio, M.F., Cochis, P.: Parameters estimation of a PEM fuel cell polarization curve and analysis of their behavior with temperature. Power Source **159**(2), 824–835 (2006)
13. Görgün, H., Arcak, M., Barbir, F.: An algorithm for estimation of membrane water content in PEM fuel cells. Power Sources **157**(1), 389–394 (2006)
14. Kundu, S.: Development and Application of a Chemical Degradation Model for Reinforced Electrolyte Membranes in Polymer Electrolyte Membrane Fuel Cells. A thesis presented to the University of Waterloo in, Chem. Eng. (2008)

15. Cheng, X., Zhang, J., Tang, Y., Song, C., Shen, J., Song, D., Zhang, J.: Hydrogen crossover in high-temperature PEM fuel cells. Power Sources **167**(1), 25–31 (2007)
16. Larminie, J.: Fuel Cell Systems Explained., Oxford Brookes University, UK, Wiley, Second edn. ISBN 0-470-84857-X (2003)
17. Bard, A.J., Faulkner, L.R.: Electrochemical Methods: Fundamentals and Applications, Second edn. Wiley, USA (2001)
18. Maggio, G., Recupero, V., Pino, L.: Modeling polymer electrolyte fuel cells: an innovative approach. Power Sources **101**(2), 275–286 (2001)
19. Chen, S., Gasteiger, H.A., Hayakawa, K., Tada, T., Shaohorn, Y.: Platinum-alloy cathode catalyst degradation in proton exchange membrane fuel cells: nanometer-scale compositional and morphological changes. Electrochem. Soc. **157**(1), 82–97 (2010)
20. Gu, W., Yu, P.T., Carter, R.N., Makharia, R., Gasteiger, H.A.: Modeling of Membrane-Electrode-Assembly Degradation in Proton-Exchange-Membrane Fuel Cells - Local H_2 Starvation and Start-Stop Induced Carbon-Support, Corrosion pp. 45–87 (2010)
21. Higashiguchi, S., Hirai, K., Shinke, N., Ibe, S., Yamazaki, O., Yasuhara, K., Hamabashiri, M., Koyama, Y., Tabata, T.: Development of Residential PEFC Cogeneration Systems at Osaka Gas. Residential Cogeneration Development Department Osaka Gas Co, Ltd (2008)
22. Fowler, M.: Degradation and reliability analysis of PEM fuel cell stacks. Chem. Eng. (2007)